Fracture mechanics analysis of arc shaped specimens for pipe grade polymers

Pemra Özbek, Christos Argyrakis and Patrick Leevers

Department of Mechanical Engineering, Imperial College London, London SW7 2AZ, UK

Abstract

Instrumented three-point bend impact fracture tests are widely used to evaluate pipe grade polymers. Often specimens cut from small-diameter pipe are used, and these are necessarily arc-shaped. Because the orientation and thermal history may differ between extruded pipe and compression moulded plaque material, this additional difference in geometry must be properly accounted for, or it may mask any effects on material properties. This paper modifies a previously published solution for the geometry-dependent energy correction factor for arc-shaped specimens, and extends it to a wider range of standard pipe geometries. When the results are properly corrected, the effects of processing on a commercial PE100 appear to be minor.

Key words: Polymer Pipe, Arc shaped specimen, Fracture, Impact, Single edge notch bend, Geometry factor, Energy correction factor, Compliance

1 Introduction

Extruded pipe is one of the most firmly established high-volume applications for a number of thermoplastics. Because even the toughest unreinforced thermoplastics are susceptible to fracture under conditions of high constraint and high strain rate, one of the most widely used criteria for evaluating them is their resistance to impact fracture. Even if impact is not the most likely of threats in service, it is regarded as imposing the most critical and decisive conditions on the material.

In Europe the most commonly used impact test method is the Charpy three-point bend impact test, using a notched straight bar specimen. For materials which fracture (rather than bending or tearing), the ISO 17281 Instrumented Charpy Test method allows the energy dissipated by the

various failure modes involved to be much more finely distinguished and quantified by geometry-independent parameters, providing a better tool for resin development. With advances in recording equipment and in the use of fracture mechanics, the data obtained are becoming more reliable, and the analysis easier. However, intrinsic mechanical filtering normally limits the impact speed to 1 m/s, which is lower than that of a pendulum Charpy test.

According to linear elastic fracture mechanics (LEFM) the impact fracture resistance (or critical strain energy release rate), G_c is given by

$$G_c = \frac{U}{BW\phi(a/W)}$$ (1)

where U is the stored energy at crack initiation, B the specimen thickness (assumed to be uniform), W is the width of the specimen in the crack growth direction and ϕ a geometry factor, related to the compliance by

$$\phi = \frac{C}{dC/d(a/W)}$$ (2)

Clearly, the reliability of G_c depends on the accuracy of $\phi(a/W)$. For straight SEN(B) specimens, $\phi(a/W)$ evaluations for various geometries are well established [1] and are tabulated in ISO 17281.

The extrusion and cooling process history during pipe production may render the properties of pipe-grade polyethylene substantially different from those of the compression or injection moulded plaques from which SEN(B) specimens are cut [2,3]. It is therefore much more relevant to test specimens cut from pipe, and for small-diameter pipe these must be arc-shaped (Fig. 1). For specimens of this shape, ϕ values are less securely established.

Niglia [4] derived an expression for the geometry factor ϕ by combining the fracture mechanics calibration functions tabulated in ASTM 399-90 with compliance results from finite element (FE) analysis. Similar methods have since been used by Nezbedová et al. [5,6] to analyse sandwich-structured specimens made from multilayer pipe. However, using Niglia's results, we determined G_c values for pipe-grade polyethylenes which differed from those using 'straight' specimens to an apparently inexplicable degree. The objective of the present study was to investigate whether the FE analysis and the boundary conditions could be made more realistic. It also seemed desirable to obtain calibrations for a wider range of pipe diameter and thickness dimensions relative to the specimen span and

depth. The dimensions of plastic pipe are defined by the outside diameter D and the *Standard Dimension Ratio* of D to minimum thickness.

2 Analysis

In LEFM, the influence of specimen geometry on fracture is treated in either of two conventional frameworks. The Irwin *stress intensity factor*,

$$K = Y\sigma\sqrt{a} \tag{3}$$

for a crack of length a depends on the applied load P and, through a dimensionless parameter Y, on the specimen geometry. For a given two-dimensional specimen shape of constant thickness B the applied load is expressed as an applied stress $\sigma = P/BX$ where X is a suitable in-plane dimension: often the length W at which the crack would meet the opposite free surface. The strain energy release rate or *crack driving force* parameter is given by the Irwin-Kies relationship

$$G = \frac{1}{2}P^2\frac{dC}{dA} \tag{4}$$

where the specimen geometry determines the functional dependence $C(a)$ of load point compliance on crack length. The K and G parameters are interrelated *via* Young's modulus (E) by

$$K^2 = E'G \tag{5}$$

where $E' = E$ under plane stress and $E' = E/(1 - v^2)$ under plane strain conditions, v being Poisson's ratio. Relating Eqs. 3 and 5 gives

$$E\frac{P^2}{2B}\frac{dC}{da} = Y^2\sigma^2 a \tag{6}$$

For the SEN(B) specimen, it is conventional to express Y in terms of the nominal surface bending stress [1] so that:

$$\sigma = \frac{3}{2}\frac{S}{W}\frac{P}{BW} \tag{7}$$

where S is the span and W is the width of the specimen. Rearranging Eq. 6 allows the Y factor to be determined from a compliance calibration

$C(a/W)$

$$Y^2 \left(\frac{a}{W} \right) = \frac{BE'}{2 \, (S/W)^2} \frac{\mathrm{d}C}{\mathrm{d}(a/W)} \tag{8}$$

where $E'BC(a/W)$ depends only on the 2D shape of the body. Alternatively, Eq. 2 can be used to determine ϕ from Y, having evaluated the compliance by integrating Eq. 8 to give

$$C = \frac{2}{BE'} \left(\frac{S}{W} \right)^2 \int Y^2 \left(\frac{a}{W} \right) \, \mathrm{d} \left(\frac{a}{W} \right) + C_0. \tag{9}$$

Here, C_0 is the integration constant, representing the uncracked compliance and can be found through finite element analysis (Table 1) or experimental measurements.

For an arc-shaped, single edge notched bend geometry, ASTM E 399-90 gives the stress intensity factor (K) in terms of two geometric functions, ($h(a/W)$ and $f(a/W)$), which are defined for two different span to width ratios ($S/W = 3$ and 4). Using these relations K can be determined by

$$K = \frac{PS}{BW^{3/2}} \left[1 + (1 - r)h \left(\frac{a}{W} \right) \right] f \left(\frac{a}{W} \right), \tag{10}$$

where r is the ratio of the inner to outer diameter of the pipe. From Eqs. 5 and 10, one can define Y by

$$Y = \frac{2}{3} \left(\frac{a}{W} \right)^{-1/2} \left[1 + (1 - r)h \left(\frac{a}{W} \right) \right] f \left(\frac{a}{W} \right) \tag{11}$$

which is used to determine compliance by Eq. 9 and hence ϕ *via* Eq. 2.

3   Calculations

The arc-shaped SEN(B) specimen geometry studied here was based on ASTM E 399-90 (Fig. 1). To evaluate the compliance of this specimen, the integral part of Eq. 9 was determined symbolically using the MATLAB 7 package. By definition, the integral constant, C_0, is the compliance of an unnotched specimen, and to determine it FE analysis was used [5,6].

Modelling of the problem included the design and evaluation of different experimental geometries. Having a variety of 8-node finite elements (shell,
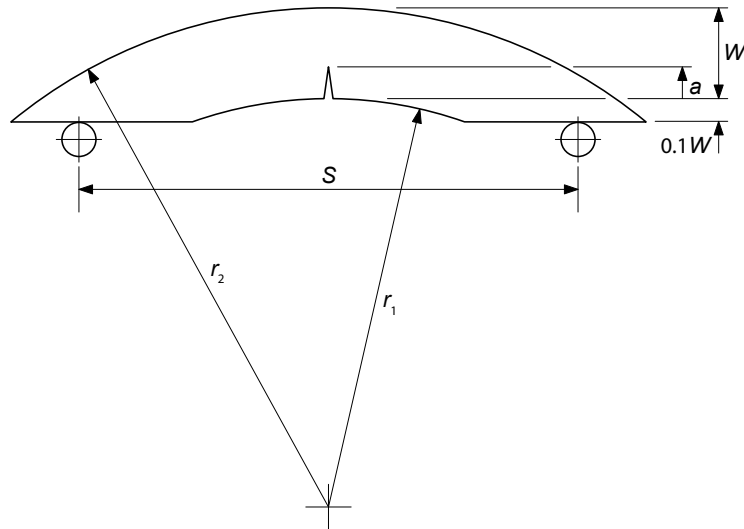
Fig. 1. Arc shaped geometry dimensions according to ASTM E 399-90

quad, plane stress) that could be applied to the current problem, it is crucial to choose a mesh which can reflect the real situation as precisely as possible. The mesh chosen was mapped, in order to have more degrees of freedom around the areas that had very small curvature. The number of elements used was 2,000 for 8-node plane stress (quad elements) and 4,000 using triangular elements. The differences between results from these two forms was very smalland by varying the number of elements (h-method) the overall compliance value changed by less than 3%. Due to symmetry, only half of the domain needed to be modelled. In the model used by Niglia [4], lateral displacements were assumed to be zero not only on the plane of symmetry (the crack plane) but also at the supports. However, polymer specimens are very compliant, and the assumption that they do not slip laterally on the support points was not supported by experimental observation. With the aim of improving the accuracy of the FE model, displacements on the support points were constrained only vertically.

Table 1
Integral Constant values, C_0EB, $a/W = 0$

	$S/W=3$	$S/W=4$	$S/W=6$
$C_0E'B$	12.8	22.6	69.6

The un-cracked compliance values are then used in Eq. 9 together with the integration function to determine ϕ according to Eq. 2. It is also possible to determine ϕ by fitting a polynomial equation to each set of FE results shown in Fig. 2. This polynomial can then be used to calculate the overall compliance value in Eq. 2 in order to determine the energy correction factor. As seen in Fig. 3, the two approaches agree well, giving confidence
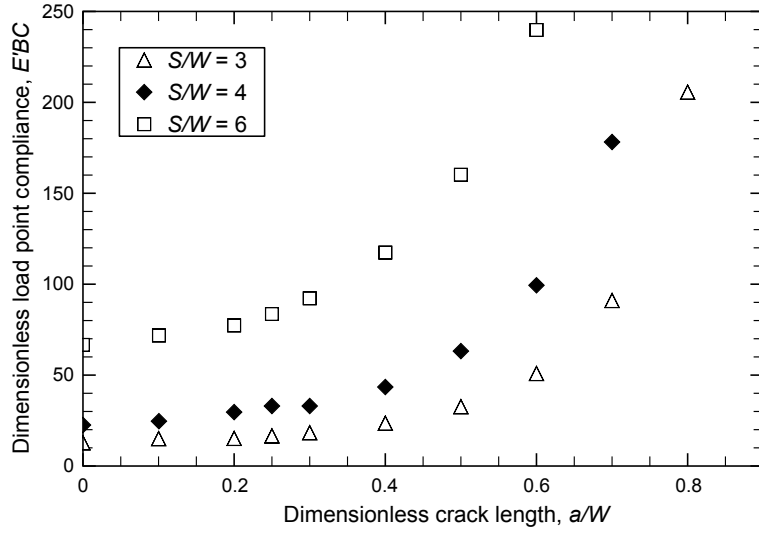
5

Fig. 2. Dimensionless compliance values computed for various S/W ratios by FE analysis

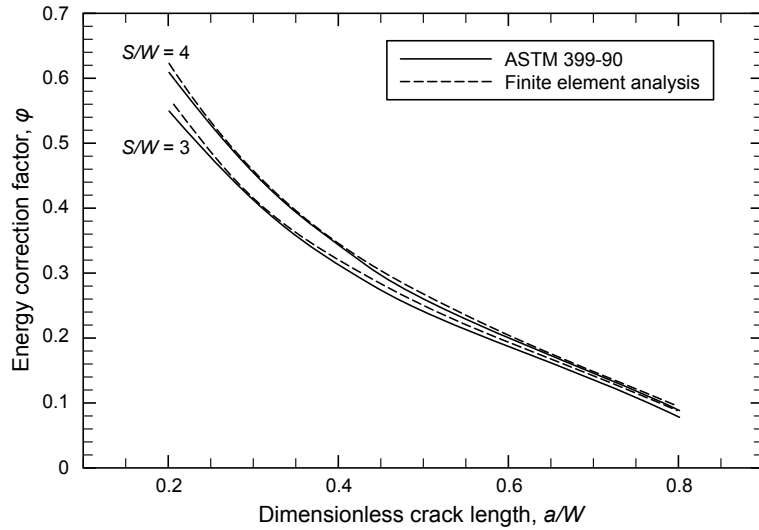in the use of FE results for further analysis.

Fig. 3. Comparison between FE approach and tabulated functions

Since the equations are defined in the standard only for two geometries ($S/W = 3$ and 4), two approaches were used to calcualte results for $S/W = 6$. The first approach was simply to linearly interpolate the coefficients of the fitting polynomial, as Williams [1] did for the original straight SEN(B) geometry. In order to check the validity of this linear exprapolation, ϕ was calculated using Eq. 2 from the overall compliance (C) of $S/W = 6$ by fitting a polynomial equation to the FE results shown in Fig. 2. Fitting the third-order polynomial

$$\phi = A_0 + A_1 \left(\frac{a}{W}\right) + A_2 \left(\frac{a}{W}\right)^2 + A_3 \left(\frac{a}{W}\right)^3 \tag{12}$$

6

to these curves gives, for SDR 11, the constants A_n shown in Table 2.

Table 2
Polynomial coefficients for Eq. 12, linearly extrapolated for $S/W = 6$

	$S/W = 3$	$S/W = 4$	$S/W = 6$
A_0	+0.99	+1.09	+1.29
A_1	−2.89	−3.15	−3.66
A_2	+3.80	+4.02	+4.44
A_3	−2.00	−2.05	−2.16

As Figure 4 shows, the ϕ values obtained by those two approaches agree reasonably well.
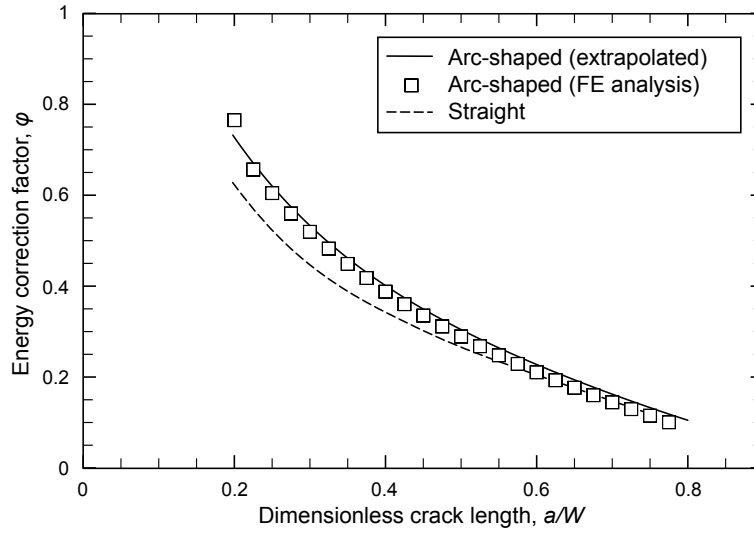

Fig. 4. Energy correction factor for straight and arc-shaped SEN(B) specimens with $S/W = 6$

Also shown on Fig. 4 is the Williams [1] energy correction factor for straight SEN(B) specimens. This emphasises that for shallow notch depths the arc shaped specimen is much more compliant than the straight specimen, due to the shallow cross section above the supports (Fig. 1), giving it greater capacity to store energy for a given G_c. As a result, we might expect the the arc-shaped specimen to show a higher transition temperature for a given material, since more ductile energy absorption will be needed to stop an unstable crack before it breaks the free surface.

Calculations were repeated for radius ratios r corresponding to standard SDR values 17.6, 13.6 and 9. The results are given in Table 3 in the dimensionless form C_0EB. The geometry factor (ϕ) was then determined as

a function of a/W for each r at S/W ratios of 3 and 4 and the results were extrapolated to $S/W = 6$, which are shown in Fig. 5.
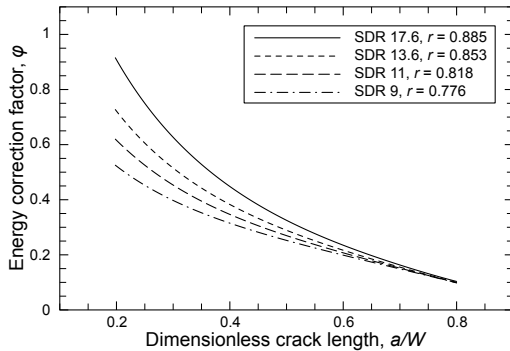
Table 3
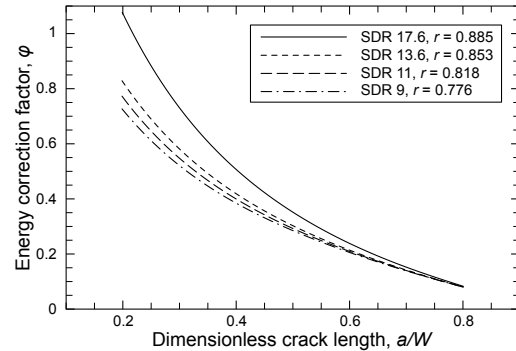Uncracked compliance of arc-shaped specimens from pipes of various geometries, C_0EB

SDR	$S/W = 3$	$S/W = 4$
9	9.10	18.6
13.6	15.1	26.9
17.6	18.1	35.1
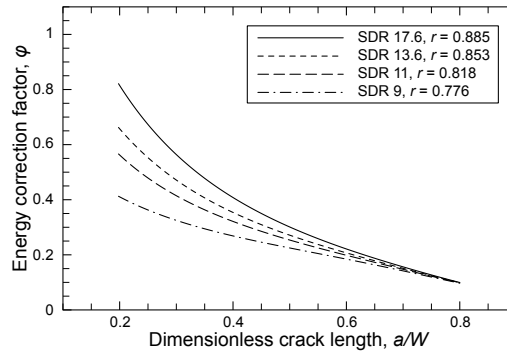
(a)

(b)

(c)

Fig. 5. Energy corrections for arc-shaped specimens of span/depth ratio (a) 3 (b) 4 and (c) 6, for diameter ratios r corresponding to pipe of various standard dimension ratios (SDR).

Figure 6 illustrates that the energy calibration factor ϕ values finally calculated here are much higher than those derived by Niglia [4], especially for small a/W ratios (short notches). This is due to the difference in boundary conditions. Releasing the spurious lateral constraints previously applied at the support points substantially increases the uncracked load-point compliance. If the support points were in fact to be laterally pinned, the lateral stress would substantially reduce the crack driving force at all notch depths: only by removing the lateral constraint is it

possible to assume that the Y factor is identical to that for a straight specimen.
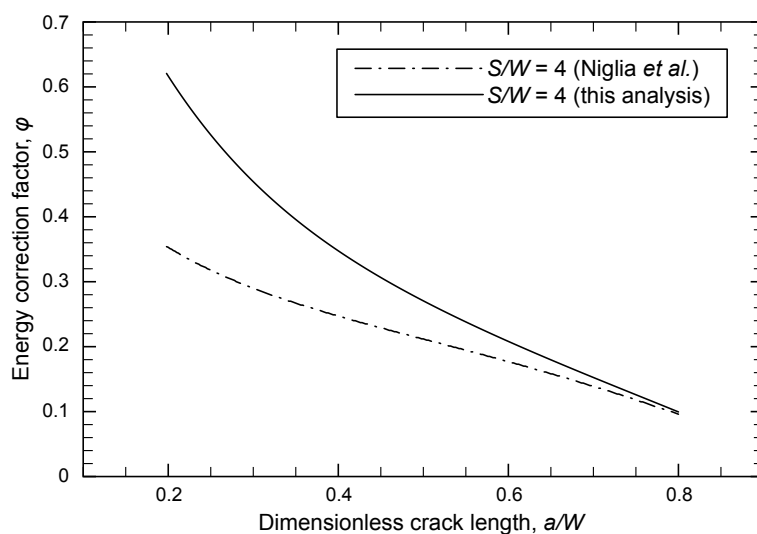

Fig. 6. Comparison of the present energy correction factor with that of Niglia [4]

4 Experimental

Using these results, the impact fracture resistance (G_c) of the same material was compared for three different SEN(B) specimen geometries: an arc-shaped one cut from commercial pipe, a compression moulded arc-shaped one and a compression moulded straight one. The objective was to distinguish the effect of processing conditions from that of specimen geometry.

A pipe-grade polyethylene of strength class PE 100, provided in granular form, was compression moulded using a hydraulically driven hot press with electrically heated platens. The material was an unpigmented modified high density (949 kg m^{-3}) grade of weight-average molecular weight 257 kg mol^{-1}. The granules were left to melt at 160°C for 25 min under low pressure, and then a pressure of 10 MPa was applied for 5 minutes in order to release trapped air and excess material. To let the crystalline phase approach its equilibrium structure, the mould was then left to cool in the machine under 10 MPa pressure until the temperature reached 60°C.

For the straight SEN(B) specimens, 12 mm thick plate was obtained by compression moulding according to ASTM standard D-1928-96. A flash type picture frame type mould of length 200 mm, width 200 mm and thickness 12 mm, with thick walls to minimise excess edge heat loss dur-

9

ing cooling, was used. From these plaques, impact bend test specimens were prepared with dimensions $B = 6$, $W = 12$ and $l = 70$ mm. For the pipe specimens, samples were directly cut from the cross section, giving an arc-shaped geometry with the dimensions of $B = 5$, $W = 10$ and $l = 70$ mm, and with the initial notch extending radially from the inside surface. To obtain arc-shaped specimens with compression-moulded material properties, a special compression mould for segment-shaped plaques was constructed, so that cooling conditions in the crack plane were essentially 'radial only'.

From these plaques, the specimens were machined to achieve an arc-shaped geometry matching the nominal dimensions of those from pipe. All specimens were notched to 25% of their thickness with a fresh razor blade, according to ISO 17281, paying attention to minimise plastic deformation near the notch. Specimens were tested according to the standard across a wide range of temperature, using a conditioning chamber for temperature control and a digital oscilloscope for data recording. For each test G_c was determined from the energy up to peak load, U_p, using Eq 1.

The results are compared in Fig. 7. The arc-shaped specimen results obtained using the original (i.e. uncorrected) ϕ calibration are not plotted; however, the amplitude of the correction now made can be inferred from 6. Results from all geometries are now broadly consistent, those from arc-shaped specimens obtained by compression moulding and from extrusion being virtually indistinguishable.
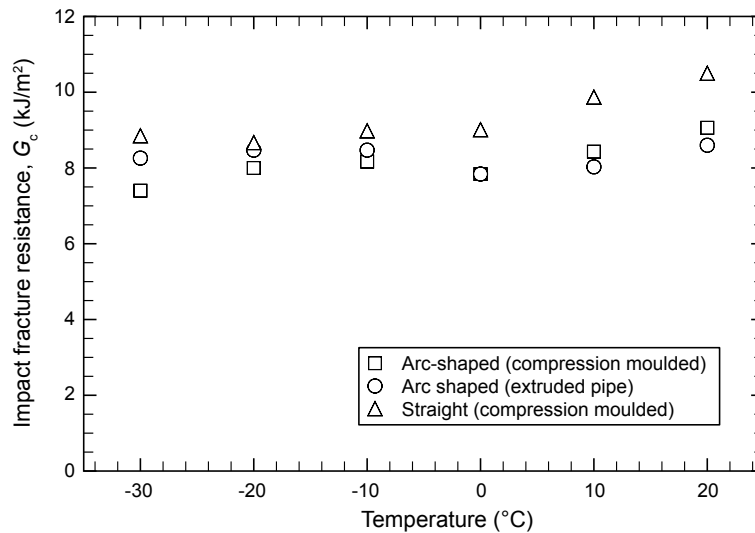

Fig. 7. Impact fracture toughness of the same PE100 material measured using three different specimen types

5 Conclusion

The determination of impact fracture resistance using instrumented impact fracture toughness testing of arc-shaped specimens according to ISO 17281 has been reviewed. New evaluations of the ISO 17281 geometry factor ϕ have been made using existing tabulated functions and new FE results for the uncracked specimen compliance, based on more realistic boundary conditions. A pipe grade polyethylene, tested using ISO 17281 and analysed using the new calibrations, showed considerably better consistency in G_c between different geometries.

References

[1] J. Williams. *Fracture Mechanics of Polymers*. Ellis Horwood, Chichester UK, 1987.

[2] P. Davis. *Process/property interactions in the new polyethylenes*. PhD thesis, University of London, 1999.

[3] R. K. Krishnaswamy, P. S. Leevers, M. J. Lamborn, A. M. Sukhadia, D. F. Register, and P. L. Maeger. Rapid crack propagation (RCP) failures in HDPE pipes: structure-property investigations. *Polymer Engineering and Science*, 46:1358–1362, 2006.

[4] J. Niglia, A. Cisilino, R. Seltzer, and P. Frontini. Determination of impact fracture toughness of polyethylene using arc-shaped specimens. *Engineering Fracture Mechanics*, 69:1391–1399, 2002.

[5] E. Nezbedová, Z. Knesl, and B. Vlach. Determination of impact fracture toughness of polyethylene using arc-shaped specimens. *Plastics, Rubber and Composites*, 36(5):207–212, 2007.

[6] J. Niglia, A. Cisilino, R. Seltzer, and P. Frontini. Determination of impact fracture toughness of polyethylene using arc-shaped specimens. *Strength of Materials*, 40(1):134–137, 2008.